Surface & Coatings Technology 259 (2014) 358–362

Contents lists available at ScienceDirect

Surface & Coatings Technology

journal homepage: www.elsevier.com/locate/surfcoat

Stress reduction of (111) homoepitaxial diamond films on nickel-coated substrate

Kun-An Chiu *, Jr-Sheng Tian, Yue-Han Wu, Chun-Yen Peng, Li Chang *

Department of Materials Science and Engineering, National Chiao Tung University, Hsinchu 300, Taiwan, ROC

ARTICLE INFO

Available online 15 March 2014

Keywords:
Homoepitaxial growth
Diamond
Nickel
CVD

ABSTRACT

Crack-free (111) homoepitaxial diamond films were grown on Ni-coated diamond substrates by microwave plasma chemical vapor deposition. After diamond deposition, the Ni islands with a size of 50–1000 nm were formed and embedded underneath the diamond films. The tensile stress in the diamond films evaluated with micro-Raman spectroscopy can be significantly reduced with the embedded Ni islands, which allows the growth of ~5 μm thick crack-free (111) homoepitaxial diamond films with a good quality, compared with those directly deposited on substrates without coating.

© 2014 Elsevier B.V. All rights reserved.

1. Introduction

Diamond has many unique physical and chemical properties including extreme hardness, the highest thermal conductivity, high breakdown field, wide band gap, high carrier mobility, high optical transmissivity, and chemical inertness [1–3]. These properties make diamond a material with high potentiality in mechanical, thermal, optical, and electrical applications. Nevertheless, natural and high-pressure high-temperature (HPHT) diamonds have limited applications due to their small dimensions and high cost. Microwave plasma chemical vapor deposition (MPCVD) is a suitable process for the synthesis of a relatively large dimension and high quality single crystal diamond. Recently, homoepitaxial diamond films grown on (001) HPHT diamonds with a high growth rate (30–150 μm/h) and large size (>1 cm^2) have been achieved [4–13]. In addition, undoped high purity (100) CVD diamond film with a thickness of 3.3 mm has been reported [14]. However, homoepitaxial growth of good crystal-quality (111) diamond film by chemical vapor deposition which may be desired for n-type doping [15] is more difficult than that of (100) because of mass formation of defects such as stacking faults and impurities. The {111}-oriented growth of homoepitaxial diamond film might promote the generation of twins and other extended defects [16]. Furthermore, many studies in the past have reported that (111) homoepitaxial diamond films tend to crack by internal stress by reason of the presence of non-diamond phases and impurities [17–19]. In general, the (111) diamond films may spontaneously crack when the film thickness is thicker than a few micrometers depending on growth conditions, and the magnitude of the stress increasing with film thickness can be up to a few GPa [18–21].

In this paper, we present a method to synthesize crack-free (111) homoepitaxial diamond films by MPCVD in that a thin nickel (Ni) layer is deposited on (111) HPHT diamond substrate before the diamond deposition. Nickel is a suitable material used upon which epitaxial diamond deposition can be applied because of its low carbon solubility (~0.2 wt.% at 900 °C) and small lattice mismatch (~1.4%) between Ni and diamond ($a_{0,\ Ni}$ = 3.517 Å, $a_{0,\ Diamond}$ = 3.567 Å).

2. Experimental details

HPHT polyhedron single crystal diamonds (size ~ 1 mm) as substrates were cleaned by using a mixing solution (HNO_3:H_2SO_4 = 1:3) for 30 min at 300 °C to remove contamination, and then the substrates were ultrasonically dipped into an acetone bath for 10 min and a methanol one for 10 min to remove residual chemical solution. Subsequently, a 20 nm thin Ni layer was deposited on one of the {111} facets of the HPHT diamond at room temperature by electron beam evaporation. The homoepitaxial growth of diamond was carried out in a 2.45-GHz MPCVD reactor. The Ni-coated substrate was placed on a Mo holder in the MPCVD reactor. The MPCVD process for diamond deposition consisted of two steps: plasma heating and homoepitaxial growth. In the first step, we used the hydrogen plasma to heat the Ni-coated substrates at 900–950 °C. In the second step of homoepitaxial growth, a gas mixture of H_2 and 0.5% CH_4 was used for plasma with a pressure at 80 Torr and the plasma power of 800–1200 W. Table 1 summarizes the deposition conditions and film thickness. The growth rate was evaluated by cross-sectional transmission electron microscopy (XTEM). The XTEM specimens were prepared by focused ion beam (FIB; FEI NOVA

* Corresponding authors at: Department of Department of Materials Science and Engineering, National Chiao Tung University, 1001, Ta-Hsueh Road, Hsinchu 300, Taiwan, ROC. Tel.: +886 3 5731615; fax: +886 3 5724727.
E-mail addresses: j73628.mse95g@nctu.edu.tw (K.-A. Chiu), lichang@cc.nctu.edu.tw (L. Chang).

http://dx.doi.org/10.1016/j.surfcoat.2014.03.012
0257-8972/© 2014 Elsevier B.V. All rights reserved.

Table 1
Diamond deposition conditions and film thickness.

Specimen no.	Deposited Ni layer (nm)	Growth time (h)	Thickness (μm)
SCD-2500	None	4	2.5
SCD-5000	None	8	5
Ni-100	20	0.17	0.1
Ni-2500	20	4	2.5
Ni-5000	20	8	5
Ni-6250	20	10	6.25

200). The epitaxy of the diamond films was confirmed by using a high-resolution X-ray diffractometer (HRXRD; Bruker Discover D8). Examinations of the presence of crack and the surface morphologies were performed by using optical microscopy (OM) and field emission scanning electron microscopy (FESEM; JEOL JSM-6500F) with X-ray energy dispersive spectroscopy (EDS). The diamond film quality and stress were assessed with micro-Raman spectroscopy (HORIBA Lab RAM HR with a 488 nm diode pump solid state laser).

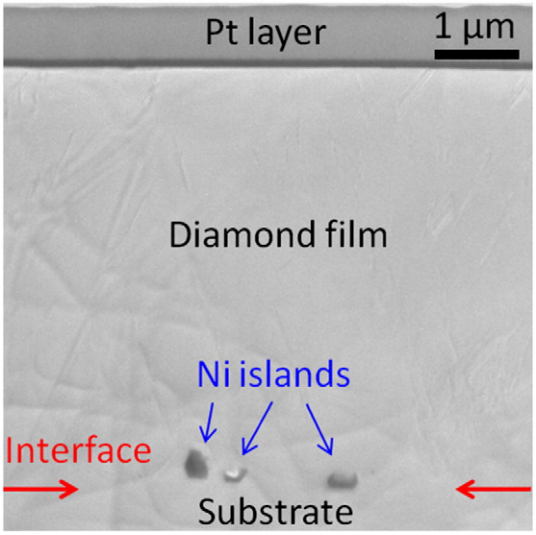

Fig. 2. Bright field cross-sectional TEM image of Ni-5000. The TEM specimen was prepared by FIB with Pt coating.

3. Results and discussion

Typical optical micrographs (OM) of (111) homoepitaxial diamond films with various thicknesses grown on HPHT and Ni-coated HPHT substrates are shown in Fig. 1. All the films exhibit a typical crystal morphology of (111) homoepitaxial diamond surface. The variations of the OM images are caused by the sensitivity of the depth of field and strong refraction of diamond during OM imaging and focus in the reflection mode. Actually, the surface roughness of these specimens examined with atomic force microscopy (AFM) is less than 20 nm. Furthermore, the diamond film thickness was determined by XTEM. Fig. 2 shows the diamond film thickness of Ni-5000 in about 5 μm with Ni islands at the interface. For surface morphology of diamond film, Fig. 1(a) shows the OM of a 2.5 μm thick diamond film directly grown on HPHT substrate (SCD-2500) without any observed cracks. For the thicker diamond film (5 μm), dense <110> cracks (indicated with black arrows) clearly appear on the surface of SCD-5000 as shown in Fig. 1(b). This phenomenon is similar to previous observations that a (111) diamond film thicker than 3.5–5 μm may crack spontaneously [19,20]. For the diamond films grown on Ni-coated HPHT substrates, no cracks can be observed on the 5 μm diamond (Ni-5000) as shown in Fig. 1(c), while the 6.25 μm diamond film (Ni-6250) clearly shows <110> cracks in Fig. 1(d) (indicated with black arrows). From the above results, the cracks in a diamond film can be suppressed by coating Ni on substrate before CVD diamond growth. Moreover, the homoepitaxy of the deposited diamond

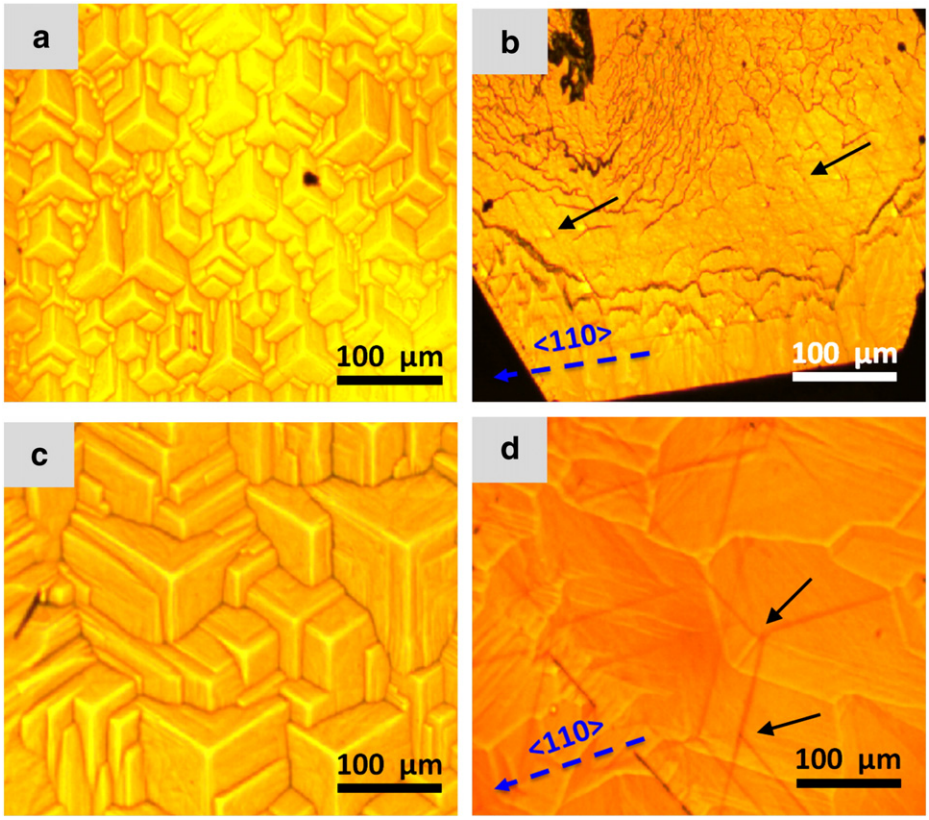

Fig. 1. Optical micrographs of (111) homoepitaxial diamond film surface of (a) SCD-2500, (b) SCD-5000, (c) Ni-5000, and (d) Ni-6250.

films with HPHT substrate can be verified with X-ray diffraction. For example, a typical XRD 2θ–ω pattern of Ni-5000 in Fig. 3(a) shows only (111) and (222) reflections, suggesting that the growth orientation of diamond film is <111>. The diamond $\left(\bar{1}11\right)$ phi-scan pattern of Ni-5000 in Fig. 3(b) shows three peaks in 120° intervals as expected for the epitaxial relationship from the 3-fold symmetry. Hence, the XRD results indicate that the 5 μm diamond film is homoepitaxially grown on the Ni-coated (111) HPHT substrate.

In order to examine the morphology of Ni layer after MPCVD, SEM observations have been done on a specimen after diamond deposition on Ni-coated substrate for 10 min. A typical SEM morphology is shown in Fig. 4(a). It can be seen that there are many hexagonal islands and small particles formed on the surface. In addition, the diamond deposits are not observed on large hexagonal islands, suggesting that the (111) homoepitaxial diamond film may be grown from the surface of the substrate covered with no Ni. These islands and particles can be identified to be Ni by energy dispersive spectroscopy (EDS) in Fig. 4(b) and X-ray diffraction analyses (not shown). It is suggested that the Ni layer in a thickness of few tens of nanometers has been changed to form hexagonal islands and particles with a size of 50–1000 nm which are dispersed on the diamond substrate after the MPCVD process. In Fig. 4(a), the triangle and hexagonal holes without nickel particles can be attributed to the strong thermal stress caused by the large difference in thermal expansion coefficient between Ni and diamond along with a weak adhesion at the interface [22] resulting in some Ni islands being peeled off and falling onto the neighboring surface areas on the diamond film after cooling. For the deposition of thicker diamond films, XTEM examinations show that the Ni-islands are encapsulated with CVD diamond.

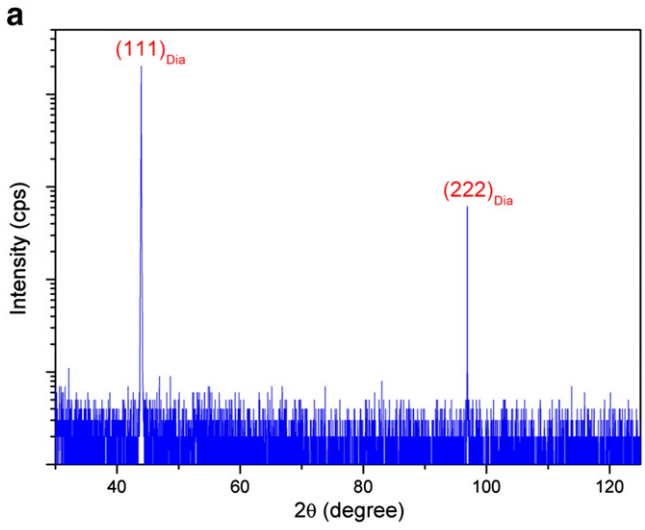

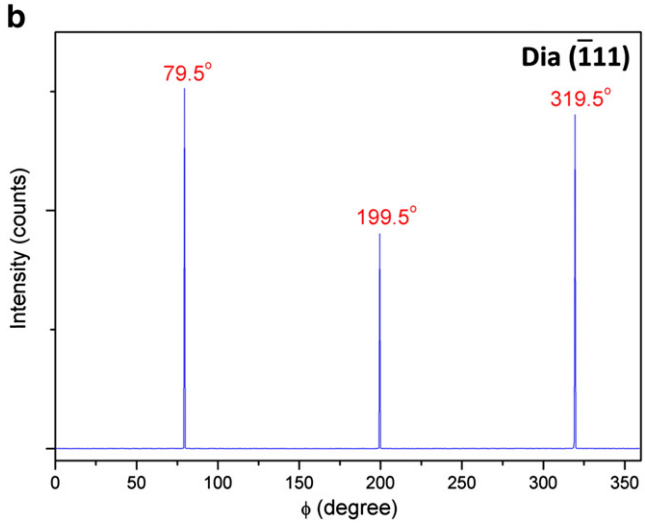

Fig. 3. XRD analyses of Ni-5000. (a) 2θ–ω pattern and (b) phi-scan pattern of the diamond $\left(\bar{1}11\right)$ reflection.

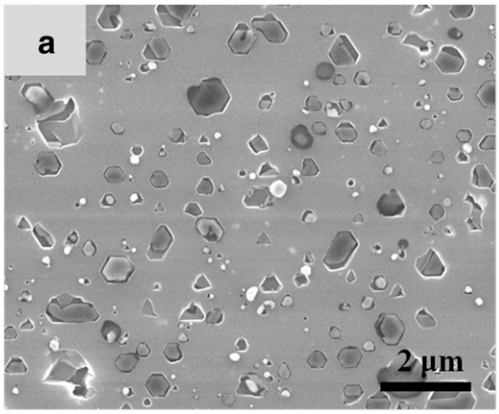

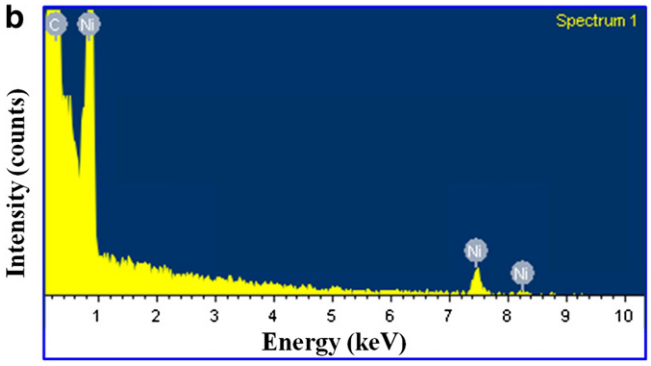

Fig. 4. (a) SEM micrograph of (111) homoepitaxial diamond film surface of Ni-100 and (b) EDS analysis of the island on diamond substrate.

Raman spectra of the samples in the 1000–1800 cm^{-1} range as shown in Fig. 5 are used to evaluate the quality of (111) homoepitaxial diamond films. Each Raman spectrum exhibits an intense diamond signal at 1332 cm^{-1} with the full width at half maximum (~2–4 cm^{-1}) close to that of the HPHT single crystal diamond, suggesting that the CVD diamond films are of high quality. There is no apparent sp^2 signal in Raman spectra in Fig. 5(b)–(e). For Fig. 5(a), very weak signals from

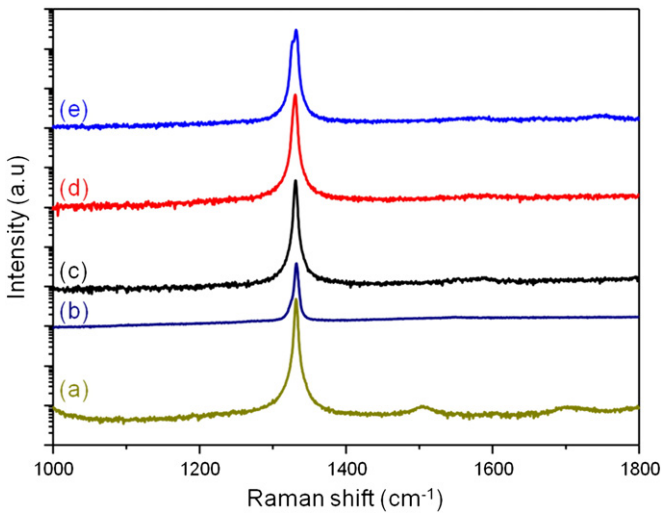

Fig. 5. Raman spectra of (111) homoepitaxial diamond films in the 1000–1800 cm^{-1} range. (a) SCD-2500, (b) SCD-5000, (c) Ni-2500, (d) Ni-5000, and (e) Ni-6250.

sp^2 bonding at ~1500 cm^{-1} and ~1700 cm^{-1} are detected due to the surface contaminants which may be resulted from carbon residues in the MPCVD chamber. Interestingly, there is no apparent graphite signal at 1580 cm^{-1} in Raman spectra of the Ni-coated samples in Fig. 5(c)–(e), which is usually observed in the case of a diamond film grown on Ni substrate as graphite may precipitate from the supersaturated nickel surface during cooling [23].

The above results show that the cracks on (111) homoepitaxial diamond films can be suppressed by coating Ni on substrate, suggesting that the stress in diamond film can be effectively reduced. It has been known that the stress can result in the shift and split of the diamond Raman peak. Further, the stress in (111) homoepitaxial diamond films can be evaluated with Raman spectroscopy as reported by Mermoux et al. [18,20,24]. Fig. 6 shows more detailed Raman spectra of the (111) homoepitaxial diamond films grown on substrates coated with and without nickel. For thin diamond films of SCD-2500 and Ni-2500 in Fig. 6(a) and (c), the peaks are apparently shifted, implying that the stresses in the films are not large. The internal stresses of SCD-2500 and Ni-2500 with a 2.5 μm thickness are determined to be smaller than 0.4 GPa after curve fitting of the peak shape. For SCD-5000, Ni-5000, and Ni-6250 which have thicker films, an apparent low-frequency shoulder signal on the left hand side of the nominal 1332.1 cm^{-1} peak can be clearly seen in SCD-5000, Ni-5000, and Ni-6250 in Fig. 6(b), (d), and (e). The presence of a low-frequency shoulder signal has been well known to be resulted from tensile stress in diamond, while a compressive stress shifts the 1332 cm^{-1} peak to a higher frequency [18–20]. Therefore, for those (111) homoepitaxial diamond films which have a downshift peak in the present cases, a high tensile stress may exist. The dependence of the stress (σ) on the shift (Δω) is

$$\sigma_{Raman} = \Delta\omega/\alpha_h[GPa]$$

where α_h is the average hydrostatic stress gauge factor [25]. Here, we use α_h of 3.2 cm^{-1}/GPa for stress calculations [18]. Comparison

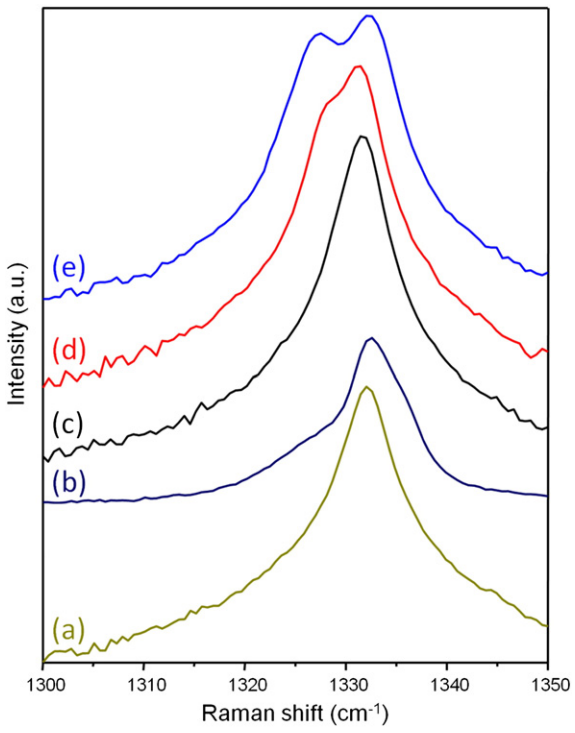

Fig. 6. Raman spectra showing the details in the 1300–1350 cm^{-1} range. (a) SCD-2500, (b) SCD-5000, (c) Ni-2500, (d) Ni-5000, and (e) Ni-6250.

Table 2
The shift (Δω) from diamond Raman peak and the corresponding stress (σ_{Raman}) in SCD-5000, Ni-5000, and Ni-6250.

Specimen no.	Δω (cm^{-1})	σ_{Raman}[a] (GPa)
SCD-5000	−5.3	+1.6
Ni-5000	−3.7	+1.1
Ni-6250	−4.7	+1.5

[a] σ_{Raman} (GPa) = Δω (cm^{-1}) / 3.2 (cm^{-1}/GPa) [18,24].

of the results from the three specimens suggests that the lower intensity of the low-frequency shoulder signal in SCD-5000 is probably due to the partial stress relaxation from the cracks. The measured shift (Δω) and the corresponding stress (σ_{Raman}) are listed in Table 2, showing that the stress increases with film thickness. For both of SCD-5000 and Ni-6250 which have cracks on their surfaces, it can be seen that their tensile stresses are higher than that of crack-free Ni-5000. Since no film delamination is observed on those two samples, the cracked film may not completely release the stress. Compared with SCD-5000 in the same diamond film thickness of 5 μm, the tensile stress in Ni-5000 is significantly reduced to about 1 GPa which may not be strong enough to result in cracking as it has been reported in literature that the tensile strength of diamond is >1.2 GPa [3]. Although the crack-free diamond film with 5 μm can be grown with embedded Ni islands, the tensile stress is seen to be rapidly increased when the thickness of diamond film exceeds 6 μm.

It has been demonstrated that the nickel islands embedded in (111) homoepitaxial diamond films can reduce the internal stress and suppress cracks. A few possible effects of the nickel islands embedded in diamond films on the stress reduction which may be worthwhile to be taken into of consideration are described in the following. First, previous studies have suggested that the grown (111) homoepitaxial diamond films tend to crack from internal stress induced by impurity and non-diamond phase such as amorphous carbon and graphite [17,18]. The growth of high-quality homoepitaxial (111) diamond film with a thickness of over 100 μm was demonstrated by using well-tuned process conditions including high microwave power, high pressure, and high purity gas [16]. The impurities and non-diamond phases may be significantly reduced in such deposition conditions. Second, Ni is much softer than diamond, so that partial stress relaxation can be done through plastic deformation in Ni. Finally, after growth, the nickel islands are shrunk quickly to develop a compressive stress in diamond during cooling due to that the thermal expansion coefficient of nickel is 10 times higher than that of diamond. The compressive stress may compensate for the tensile stress in the diamond film, such that low residual tensile stress exists in the diamond film with embedded nickel islands. Further investigations need to be done to clarify the above possible effects.

4. Conclusions

In this work, Ni coating on (111) HPHT diamond substrates can result in the growth of thick crack-free homoepitaxial diamond films by microwave plasma chemical vapor deposition. Formation of Ni hexagonal islands in hundreds of nanometers occurs in the early stage of diamond deposition. Examinations of the surface of 5 μm homoepitaxial diamond films on Ni-coated substrate show no crack formation, while cracks are clearly observed on the surface of the same thick diamond film directly deposited on the substrate without Ni coating. From the diamond Raman peak shift, the evaluated tensile stress in the CVD diamond film on Ni-coated substrate can be significantly reduced with the embedded nickel islands in comparison with the stress in the film grown on substrate without Ni coating.

Acknowledgments

This work was supported by the National Science Council Taiwan under contract of NSC 101-2221-E-009-049-MY3.

References

[1] H. Liu, D.S. Dandy, Diamond Chemical Vapor Deposition: Nucleation and Early Growth Stages, Noyes, 1995.
[2] K. Kobashi, Diamond films—Chemical Vapor Deposition for Oriented and Heteroepitaxial Growth, Elsevier, 2005, ISBN 0080447236. 300.
[3] K.E. Spear, J.P. Dismukes, Synthetic Diamond: Emerging CVD Science and Technology, Wiley-Interscience, 1994. 4.
[4] C.S. Yan, Y.K. Vohra, H.K. Mao, R.J. Hemley, Proc. Natl. Acad. Sci. U. S. A. 99 (2002) 12523.
[5] C.S. Yan, H.K. Mao, W. Li, J. Qian, Y. Zhao, R.J. Hemley, Phys. Status Solidi A 201 (2004) 25–27.
[6] Q. Zhang, H.D. Li, S.H. Cheng, Q.L. Wang, L.A. Li, X.Y. Lv, G.T. Zou, Diam. Relat. Mater. 20 (2011) 496–500.
[7] A. Chayahara, Y. Mokuno, Y. Horino, Y. Takasu, H. Kato, H. Yoshikawa, N. Fujimori, Diam. Relat. Mater. 13 (2004) 1954–1958.
[8] Y. Mokuno, A. Chayahara, Y. Soda, Y. Horino, N. Fujimori, Diam. Relat. Mater. 14 (2005) 1743–1746.
[9] A. Tallaire, J. Achard, F. Silva, R.S. Sussmann, A. Gicquel, Diam. Relat. Mater. 14 (2005) 249–254.
[10] H. Yamada, A. Chayahara, Y. Mokuno, N. Tsubouchi, S.I. Shikata, N. Fujimori, Diam. Relat. Mater. 20 (2011) 616–619.
[11] H. Yamada, A. Chayahara, Y. Mokuno, H. Umezawa, S.I. Shikata, N. Fujimori, Appl. Phys. Express 3 (2010) 051301.
[12] H. Yamada, A. Chayahara, H. Umezawa, N. Tsubouchi, Y. Mokuno, S.I. Shikata, Diam. Relat. Mater. 24 (2012) 29–33.
[13] Y. Mokuno, A. Chayahara, H. Yamada, N. Tsubouchi, Diam. Relat. Mater. 18 (2009) 1258–1261.
[14] B. Willems, A. Tallaire, J. Achard, Diam. Relat. Mater. 41 (2014) 25–33.
[15] N. Casanova, A. Tajani, E. Gheeraert, E. Bustarret, J.A. Garrido, C.E. Nebel, M. Stutzmann, Diam. Relat. Mater. 11 (2002) 328–331.
[16] A. Tallaire, J. Achard, A. Boussadi, O. Brinza, A. Gicquel, I.N. Kupriyanov, Y.N. Palyanov, G. Sakr, J. Barjon, Diam. Relat. Mater. 41 (2014) 34–40.
[17] I. Sakaguchi, M. Nishitani-Gamo, K.P. Loh, S. Hishita, H. Haneda, Appl. Phys. Lett. 73 (1998) 2675–2677.
[18] M. Mermoux, B. Marcus, A. Crisci, A. Tajani, E. Gheeraert, E. Bustarret, Diam. Relat. Mater. 13 (2004) 329–334.
[19] C.J. Chu, M.P.D. Evelyne, R.H. Hauge, J.L. Margrave, J. Appl. Phys. 70 (1991) 1695–1705.
[20] M. Mermoux, B. Marcus, A. Crisci, A. Tajani, E. Gheeraert, E. Bustarret, J. Appl. Phys. 97 (2005) 043530.
[21] I. Sakaguchi, M. Nishitani-Gamo, K.P. Loh, H. Haneda, T. Ando, Diam. Relat. Mater. 8 (1999) 1291–1295.
[22] R. Ramesham, M.F. Rose, R.F. Askew, Surf. Coat. Technol. 79 (1996) 55–66.
[23] W. Zhu, P.C. Yang, J.T. Glass, Appl. Phys. Lett. 63 (12) (1993) 1640–1642.
[24] M. Mermoux, A. Tajani, B. Marcus, E. Bustarret, E. Gheeraert, M. Nesladek, S. Koizumi, Diam. Relat. Mater. 13 (2004) 886–890.
[25] Y. Kato, H. Umezawa, S.I. Shikata, T. Teraji, Diam. Relat. Mater. 23 (2012) 109–111.